

Magnetar-like X-ray Bursts from an Anomalous X-ray Pulsar

F. P. Gavriil*, V. M. Kaspi*[†], P. M. Woods[‡]

* Physics Department, McGill University, Montreal, QC H3W 2C4, Canada

[†] MIT Department of Physics and Center for Space Research, Cambridge, MA 02139, USA

[‡] Space Science Research Center, National Space Science and Technology Center, Huntsville, AL 35805, USA; Universities Space Research Association

Anomalous X-ray Pulsars (AXPs) are a class of rare X-ray pulsars whose energy source has been perplexing for some 20 years^{1,2,3}. Unlike other, better understood X-ray pulsars, AXPs cannot be powered by rotation or by accretion from a binary companion, hence the designation “anomalous.” AXP rotational and radiative properties are strikingly similar to those of another class of exotic objects, the Soft Gamma Repeaters (SGRs). However, the defining property of SGRs, namely their low-energy gamma-ray and X-ray bursts, have heretofore not been seen in AXPs. SGRs are thought to be “magnetars,” young neutron stars powered by the decay of an ultra-high magnetic field^{4,5}. The suggestion that AXPs are magnetars has been controversial⁶. Here we report the discovery, from the direction of AXP 1E 1048–5937, of two X-ray bursts that have many properties similar to those of SGR bursts. These events imply a close relationship between AXPs and SGRs, with both being magnetars.

SGRs are believed to be magnetars because the high magnetic field provides the torque for their rapid spin-down, as well as the energy to power their bursts and quiescent X-ray emission⁴. AXPs have been suggested to be magnetars, albeit less active, because of their similar spin periods, rates of spin down, location in the Galactic plane, and similar though somewhat softer X-ray spectra to those of SGRs in quiescence⁷. The physical difference between the two classes is unknown, but, in the magnetar model, is likely related to the magnitude or distribution of the stellar magnetic field. However, the apparent absence of any bursting behavior in AXPs has led to suggestions that they could be powered, not by magnetism, but by accretion from a disk of material remaining after the

birth supernova event⁶. If so, the observational similarities between AXPs and SGRs must be purely coincidental.

A program to regularly monitor the AXPs using the Proportional Counter Array (PCA)⁸ aboard NASA's *Rossi X-ray Timing Explorer (RXTE)* was begun in 1996 in order to determine their long-term timing, pulsed flux, and pulse profile stabilities^{9,10,11,12}. As part of this program, motivated by the existence of SGR bursts, we also searched the AXP data for bursts (see Fig. 1 caption for details).

We discovered two highly significant bursts from the direction of AXP 1E 1048–5937 in this way. The first (hereafter Burst 1) occurred during a 3-ks PCA observation obtained on 2001 October 29 with chance probability $P \simeq 6 \times 10^{-18}$ after accounting for the number of trials. A second burst (hereafter Burst 2) was found in a 3-ks observation obtained on 2001 November 14, with analogous probability $P \simeq 2 \times 10^{-9}$. No other significant bursts were found toward 1E 1048–5937. The total PCA time searched for bursts toward this source was 380 ks in observations obtained from 1996–2002.

The burst profiles are shown in Figure 1. Both are characterized by fast rises and slow decays (see Table 1). Burst 1 appears to have a long, low-level tail that is just above the PCA background as determined by intervals selected before and after the bursts (see Fig. 1), while Burst 2 is much shorter. Both bursts arrived at the peak of the AXP pulse within uncertainties in burst arrival time and definition of pulse peak. The probability of this occurring by random chance is $\sim 1\%$. We note a marginal ($\sim 3\sigma$) increase in the pulsed flux from 1E 1048.1–5937 that commenced with the observation in which Burst 1 was detected, and which lasted ~ 4 weeks.

To determine the bursts' spectral properties, we first established that neither burst exhibited significant spectral evolution with time by computing hardness ratios (the ratio of 10–60 keV counts to 2–10 keV counts) for the first 0.5-s and subsequent 1.5-s burst intervals. No significant change in hardness was detected, though marginal spectral softening with time was detected after the first 2.5 s of Burst 1. Hardness ratios for Burst 1 and 2 for the 1 s after burst onset were 2.8 ± 0.8 and 1.0 ± 0.3 , respectively.

We then fit the spectra from the first 1 s of each burst to two one-component models, a power law and a black body (see Table 1). Continuum models provided an adequate characterization of the Burst 2 spectrum but not of the Burst 1 spectrum. As seen in Figure 2, the spectrum for the 1 s after the Burst 1 onset exhibits a feature near 14 keV. This feature is clear in all binning schemes and

is prominent throughout the first ~ 1 s of the burst. No known PCA instrumental effect produces a feature at this energy (K. Jahoda, personal communication).

Due to the wide ($\sim 1^\circ$) field-of-view (FOV) and lack of imaging capabilities of the PCA, we cannot verify that the bursts originated from the location of the AXP. The low peak X-ray fluxes of the events (see Table 1) preclude determining the source’s location using data from other, better imaging instruments that were contemporaneously observing the X-ray sky, such as the *RXTE* All Sky Monitor, or the Wide Field Camera aboard *BeppoSAX*. We must therefore consider other possible origins from the bursts before concluding they were from the AXP.

The bursts’ short rise times (Table 1) require emission regions of less than a few thousand km, implying a compact object origin. So-called Type I X-ray bursts are a well-studied phenomenon that result from unstable helium burning just below the surface of a weakly magnetized neutron star that is accreting material in a low-mass X-ray binary (LMXB)¹³. However, Type I bursts from an LMXB in the same FOV as 1E 1048.1–5937 are unlikely to explain our observed bursts because (i) the burst rise times are much shorter than those of Type I bursts; (ii) the burst spectra are much harder than those of Type I bursts; (iii) Burst 2 shows no evidence for spectral softening with time and no Type I burst has ever exhibited a spectral feature like the one detected in Burst 1; (iv) the bursts are extremely faint, implying a source location well outside the Milky Way for Type I burst luminosities (v) there are no known LMXBs in the FOV¹⁴. Type II X-ray bursts¹³ are a much rarer and less well understood phenomenon observed thus far in only two sources, both accreting binaries. The bursts we have observed are unlikely to be Type II bursts from an unknown X-ray binary in the PCA FOV because (i) of the rarity of such events; (ii) Type II bursts have longer rise times than do our bursts; (iii) no Type II burst has exhibited a spectral feature like that seen in Burst 1.

Classical gamma-ray bursts (GRBs) sometimes exhibit prompt X-ray emission that can have temporal and spectral signatures similar to those we have observed¹⁵. However, the likelihood of two GRBs occurring within 1° of each other is small, and GRBs are not known to repeat. Conservatively assuming GRB spectral model parameters that result in low gamma-ray fluxes and extrapolating the GRB rate¹⁶ as measured with the Burst and Transient Source Experiment (BATSE)¹⁷ assuming homogeneity below the BATSE threshold, we estimate a probability that these events are unrelated GRBs that occurred by chance in the same *RXTE* FOV during our 1E 1048.1–5937 monitoring

observations (conservatively neglecting that they occurred within two weeks of each other) of $\sim 9 \times 10^{-5}$.

The observed burst properties are in many ways similar to those seen from SGRs¹⁸. The fast rise and slow decay profiles are consistent with SGR time histories, as are the burst durations (neglecting the long, low-level tail of Burst 1). Both AXP and SGR bursts are spectrally much harder than is their quiescent pulsed emission. The burst peak fluxes and fluences fall within the range seen for SGRs, and the spectrum of Burst 2 is consistent with SGR burst spectra of comparable fluence. Burst 1 has characteristics unlike nearly all SGR bursts, specifically its long tail and spectral feature. However, we note that a single event from SGR 1900+14 was shown^{19,20} to possess each of these properties. The marginal increase in the pulsed fraction that we observed at the burst epochs is consistent with SGR pulsed flux increases seen during bursting episodes²¹. Finally, the fact that in spite of several years of monitoring, the only two bursts detected occurred within two weeks of each other suggests episodic bursting activity, the hallmark of SGRs. Thus, the characteristics of these events match the burst properties of SGRs far better than any other known burst phenomenon.

In the magnetar model for SGRs^{4,7}, bursts are a result of sudden crustal yields due to stress from the outward diffusion of the huge internal magnetic field. Such yields cause crust shears which twist the external magnetic field, releasing energy. Thompson & Duncan⁷ who, upon suggesting that AXPs are also magnetars, predicted X-ray bursts should eventually be seen from them. By contrast, in no AXP accretion scenario, whether binary or isolated fall-back disk, are SGR-like bursts expected.

The large 14-keV spectral line in Burst 1 is intriguing. An electron cyclotron feature at this energy E implies a magnetic field of $B = 2\pi mcE/he \simeq 1.2 \times 10^{12}$ G (where m is the electron mass, c is the speed of light, h is Planck's constant, and e is the electron charge), while a proton cyclotron feature implies $B \simeq 2.4 \times 10^{15}$ G. The former is significantly lower than is implied from the source's spin-down and is typical of conventional young neutron stars, rather than magnetars. The latter is higher than is implied by the spin-down yet reasonable for the magnetar model as the spin-down torque is sensitive only to the dipolar component of the magnetic field.

Why do the burst rates of AXPs and SGRs differ so markedly, in spite of their common magnetar nature? One possibility is that AXP internal magnetic fields are much larger than those of SGRs; if so, AXP crusts can undergo plastic deformation rather than brittle fracturing⁷. However, this is opposite to what is inferred from the two classes' spin-down rates, suggesting the latter is an unreliable

internal field indicator. This could help reconcile the contrasting radiative properties of AXPs and apparently high-magnetic field radio pulsars²². It also suggests that AXPs are SGR progenitors, with bursting behavior commencing as the field decays. This is consistent with the smaller AXP ages implied by their more numerous associations with supernova remnants²³, but does not explain why AXPs and SGRs have similar spin period distributions, since AXPs spin down as they age²⁴. This aspect of magnetar physics remains a puzzle.

Received 3 November 2018; Accepted **draft**.

1. Fahlman, G. G. & Gregory, P. C. An X-ray pulsar in SNR G109.1–1.0. *Nature*, **293**, 202–204 (1981).
2. van Paradijs, J., Taam, R. E. & van den Heuvel, E. P. J. On the nature of the ‘anomalous’ 6-s X-ray pulsars. *Astron. Astrophys.*, **299**, L41–L44 (1995).
3. Mereghetti, S. & Stella, L. The very low mass X-ray binary pulsars: A new class of sources? *Astrophys. J.*, **442**, L17–L20 (1995).
4. Thompson, C. & Duncan, R. C. The soft gamma repeaters as very strongly magnetized neutron stars - I. Radiative mechanism for outbursts. *Mon. Not. R. Astron. Soc.*, **275**, 255–300 July 1995.
5. Kouveliotou, C., Dieters, S., Strohmayer, T., van Paradijs, J., Fishman, G. J., Meegan, C. A., Hurley, K., Kommers, J., Smith, I., Frail, D. & Murakami, T. An X-ray pulsar with a superstrong magnetic field in the soft γ -ray repeater SGR 1806–20. *Nature*, **393**, 235–237 (1998).
6. Chatterjee, P., Hernquist, L. & Narayan, R. An accretion model for anomalous X-ray pulsars. *Astrophys. J.*, **534**, 373 (2000).
7. Thompson, C. & Duncan, R. C. The soft gamma repeaters as very strongly magnetized neutron stars. II. Quiescent neutrino, x-ray, and alfvén wave emission. *Astrophys. J.*, **473**, 322–342 (1996).
8. Jahoda, K., Swank, J. H., Giles, A. B., Stark, M. J., Strohmayer, T., Zhang, W. & Morgan, E. H. In-orbit performance and calibration of the Rossi X-ray Timing Explorer (RXTE) proportional counter array (pca). *Proc. SPIE*, **2808**, 59 (1996).
9. Kaspi, V. M., Chakrabarty, D. & Steinberger, J. Phase-coherent timing of two anomalous X-ray pulsars. *Astrophys. J.*, **525**, L33–L36 (1999).
10. Kaspi, V. M., Lackey, J. R. & Chakrabarty, D. A glitch in an anomalous X-ray pulsar. *Astrophys. J.*, **537**, L31–L34 (2000).
11. Kaspi, V. M., Gavril, F. P., Chakrabarty, D., Lackey, J. R. & Munro, M. P. Long-term RXTE monitoring of the anomalous X-ray pulsar 1E 1048.1–5973. *Astrophys. J.*, **558**, 253–262 (2001).

12. Gavriil, F. P. & Kaspi, V. M. Long-Term Rossi X-Ray Timing Explorer Monitoring of Anomalous X-Ray Pulsars. *Astrophys. J.*, **567**, 1067–1076 (2002).
13. Lewin, W. H. G., Van Paradijs, J. & Taam, R. E. in *X-Ray Binaries* (eds Lewin, W. H. G., van Paradijs, J. & van den Heuvel, E. P. J.) 175–232 (Cambridge University Press, Cambridge, 1995).
14. Liu, Q. Z., van Paradijs, J. & van den Heuvel, E. P. J. A catalogue of low-mass X-ray binaries. *Astron. Astrophys.*, **368**, 1021–1054 (2001).
15. Heise, J., in't Zand, J., Kippen, M. & Woods, P. (Memorie della Societa' Astronomica Italiana, 2001). <http://xxx.lanl.gov/abs/astro-ph/0111246>.
16. Stern, B. E., Tikhomirova, Y., Kompaneets, D., Svensson, R. & Poutanen, J. An Off-Line Scan of the BATSE Daily Records and a Large Uniform Sample of Gamma-Ray Bursts. *Astrophys. J.*, **563**, 80–94 (2001).
17. Fishman, G. J. et al. Overview of observations from BATSE on the Compton observatory. *Astron. Astrophys. Supp.* **97**, 17–20 (1993).
18. Göğüş, E., Kouveliotou, C., Woods, P. M., Thompson, C., Duncan, R. C. & Briggs, M. S. Temporal and Spectral Characteristics of Short Bursts from the Soft Gamma Repeaters 1806-20 and 1900+14. *Astrophys. J.*, **558**, 228–236 (2001).
19. Ibrahim, A. I., Strohmayer, T. E., Woods, P. M., Kouveliotou, C., Thompson, C., Duncan, R. C., Dieters, S., Swank, J. H., van Paradijs, J. & Finger, M. An Unusual Burst from Soft Gamma Repeater SGR 1900+14: Comparisons with Giant Flares and Implications for the Magnetar Model. *Astrophys. J.*, **558**, 237–252 (2001).
20. Strohmayer, T. E. & Ibrahim, A. I. Discovery of a 6.4 KEV Emission Line in a Burst from SGR 1900+14. *Astrophys. J.*, **537**, L111–L114 (2000).
21. Woods, P. M., Kouveliotou, C., Göğüş, E., Finger, M. H., Swank, J., Smith, D. A., Hurley, K. & Thompson, C. Evidence for a Sudden Magnetic Field Reconfiguration in Soft Gamma Repeater 1900+14. *Astrophys. J.*, **552**, 748–755 (2001).
22. Pivovarov, M., Kaspi, V. M. & Camilo, F. X-ray observations of the high magnetic field radio pulsar PSR J1814–1744. *Astrophys. J.*, **535**, 379–384 (2000).
23. Gotthelf, E. V., Vasisht, G. & Dotani, T. On the Spin History of the X-Ray Pulsar in Kes 73: Further Evidence for an Ultramagnetized Neutron Star. *Astrophys. J.*, **522**, L49–L52 (1999).
24. Gaensler, B. M., Slane, P. O., Gotthelf, E. V. & Vasisht, G. Anomalous X-Ray Pulsars and Soft Gamma-Ray Repeaters in Supernova Remnants. *Astrophys. J.*, **559**, 963–972 (2001).

25. Tiengo, A., Göhler, E., Staubert, R. & Mereghetti, S. The anomalous X-ray pulsar 1E 1048.1-5937: Phase resolved spectroscopy with the XMM-Newton satellite. *Astron. Astrophys.*, **383**, 182–187 (2002).
 26. Arnaud, K. A. in *Astronomical Data Analysis Software and Systems V* (eds Jacoby, G. & Barnes, J.) 17 (ASP, San Francisco, 1996).
-

Acknowledgements

We thank E. Kuulkers, K. Hurley, K. Jahoda, C. Kouveliotou, W. Lewin, M. Lyutikov, M. Munro, D. Psaltis, S. Ransom, M. Roberts, D. Smith, and C. Thompson for useful discussions. This work was supported in part by a NASA LTSA grant, an NSERC Research Grant, and an NSF Career Award. VMK is a Canada Research Chair and an Alfred P. Sloan Fellow. This research has made use of data obtained through the High Energy Astrophysics Science Archive Research Center Online Service, provided by the NASA/Goddard Space Flight Center.

Correspondence and requests for materials should be addressed to vkaspi@physics.mcgill.ca.

Table 1	AXP Burst Timing and Spectral Properties	
	Burst 1	Burst 2
Temporal Properties		
Burst day, (MJD)	52211	52227
Burst start time, (fraction of day, UT)	0.2301949(24)	0.836323379(68)
Burst rise time, t_r (ms)	21^{+9}_{-5}	$5.9^{+2.0}_{-1.2}$
Burst duration, T_{90} (s)	51^{+28}_{-19}	$2.0^{+4.9}_{-0.7}$
Burst phase	-0.018 ± 0.034	0.051 ± 0.032
Fluxes and Fluences		
T_{90} fluence (counts)	485 ± 118	101 ± 15
T_{90} fluence ($\times 10^{-10}$ erg cm $^{-2}$)	20.3 ± 4.8	5.3 ± 1.2
1-s fluence (counts)	117 ± 13	69 ± 10
1-s fluence ($\times 10^{-10}$ erg cm $^{-2}$)	$5.9^{+8.6}_{-1.9}$	$4.0^{+3.5}_{-0.8}$
Peak flux for 64 ms ($\times 10^{-10}$ erg s $^{-1}$ cm $^{-2}$)	31^{+45}_{-10}	26^{+23}_{-5}
Peak flux for t_r ms ($\times 10^{-10}$ erg s $^{-1}$ cm $^{-2}$)	54^{+79}_{-17}	114^{+100}_{-23}
Spectral Properties		
Power law:		
power law index	$0.89^{+1.8}_{-0.71}$	$1.38^{+0.75}_{-0.62}$
power law flux ($\times 10^{-10}$ erg s $^{-1}$ cm $^{-2}$)	$2.0^{+8.4}_{-1.8}$	$4.0^{+3.5}_{-0.8}$
line energy (keV)	13.9 ± 0.9	...
line width, σ (keV)	$2.2^{+1.3}_{-1.0}$...
line flux ($\times 10^{-10}$ erg s $^{-1}$ cm $^{-2}$)	$3.9^{+2.2}_{-1.6}$...
reduced χ^2 /degrees of freedom	1.24/15	0.77/5
Black body:		
kT (keV)	$3.9^{+3.7}_{-2.7}$	$3.6^{+2.2}_{-1.3}$
black body flux ($\times 10^{-10}$ erg s $^{-1}$ cm $^{-2}$)	$2.4^{+5.0}_{-2.1}$	$3.8^{+3.3}_{-1.5}$
line energy (keV)	$14.2^{+1.1}_{-1.2}$...
line width (keV)	$2.1^{+1.5}_{-1.3}$...
line flux ($\times 10^{-10}$ erg s $^{-1}$ cm $^{-2}$)	$3.7^{+2.2}_{-1.9}$...
reduced χ^2 /degrees of freedom	1.23/15	1.66/5

Table Caption

Table 1. The uncertainty on the burst start time is the burst rise time t_r and is given in parenthesis as the uncertainty in the last digits shown. The burst rise times were determined by a maximum likelihood fit to the unbinned data using a piecewise function having a linear rise and exponential decay. The burst duration, T_{90} , is the interval between when 5% and 95% of the total 2–20 keV burst fluence was received. The background regions used for both the duration and spectral analyses are shown in Figure 1. Burst phase is defined such that the peak of the periodic pulsation is at phase 0/1. All fluences and fluxes are in the 2–20 keV range. T_{90} fluences in cgs units were calculated assuming a power-law spectral model and spectral grouping that demanded a minimum of 20 counts per spectral bin. The 1-s fluences in cgs units correspond to the fluxes found in the spectral modeling. The spectral rebinning method used in all spectral modeling for Burst 1 was to group the 256 PCA channels by a factor of 4, while for Burst 2, we demanded at least 20 counts per spectral bin. Peak fluxes on the short time scales were determined by scaling the 1-s fluxes by number of counts. For all spectral fits, the equivalent neutral hydrogen column density was held fixed at $1.2 \times 10^{22} \text{ cm}^{-2}$, the value determined from recent XMM observations²⁵. Spectral fits were determined for the first 1 s after the burst start times. Spectral modeling was done using photons in the 2–40 keV range. Response matrices were created using the FT00L `pcarsp`¹. Uncertainties in the Table are 68% confidence intervals, except for those reported for the cgs-unit fluences and fluxes, as well as the spectral model parameters, for which we report 90% confidence intervals.

¹http://heasarc.gsfc.nasa.gov/docs/xte/recipes/pca_response.html

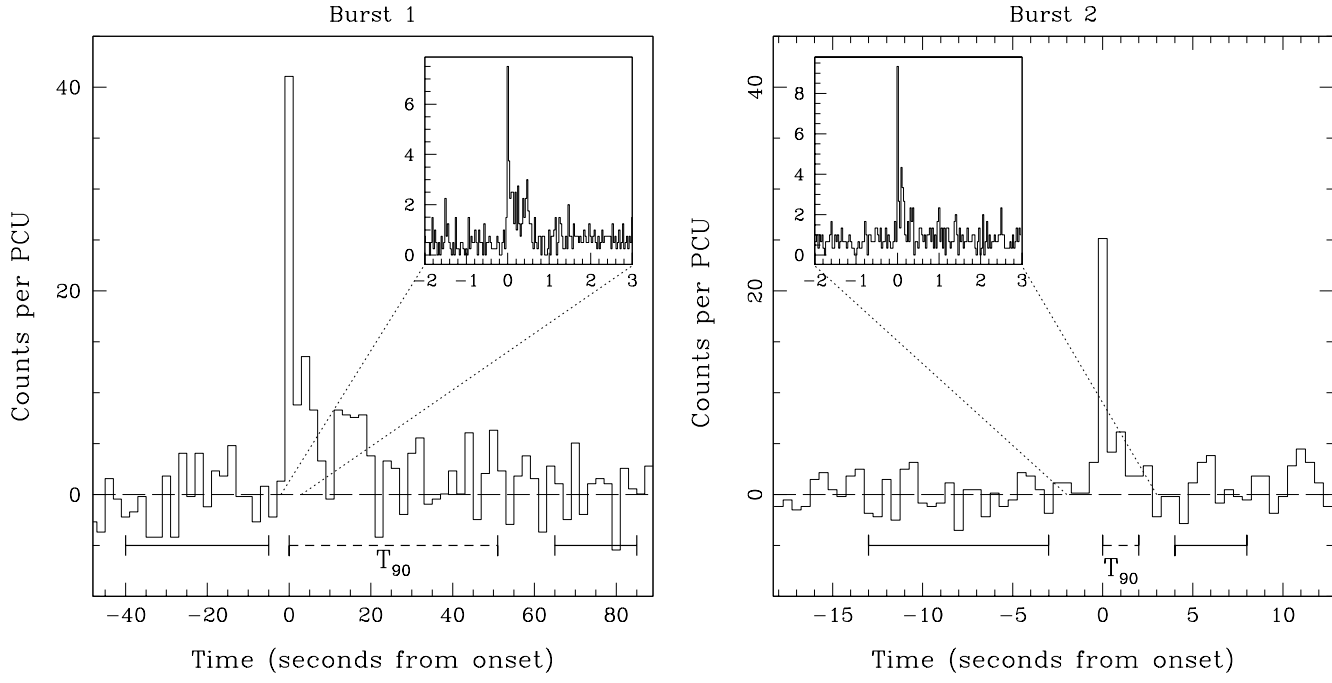
**Figure 1.**

Figure 1 Caption

Lightcurves for the observed bursts. The *RXTE* AXP data set consists of short (~ 3 ks) snapshots, as well as longer archival observations, all taken in the PCA **GoodXenonwithPropane** mode, which records photon arrival times with 1- μ s resolution, and bins photon energies into 256 channels. Time series were initially created with 31.25-ms resolution from photons having energies in the range 2–20 keV for each PCA Proportional Counter Unit (PCU) separately, using all xenon layers. Photon arrival times at each epoch were adjusted to the solar system barycentre. The resulting time series were searched for significant excursions from the mean count rate by comparing each time bin value with a windowed 7-s running mean. Bursts were identified assuming Poissonian statistics, and by combining probabilities from the separate PCUs. Left Panel: Background subtracted 2-20 keV light curves for Burst 1, displayed with 2-s time resolution. The solid horizontal lines before and after the bursts are the boundaries of the pre- and post-background intervals used for calculating T_{90} and for spectral modeling. The T_{90} interval is shown as a horizontal dashed line. Right Panel: Same but for Burst 2, and with 0.5-s time resolution in the main panel. The insets show the peak of each burst with 31.25-ms time resolution. We verified that there was no significantly enhanced signal from PCA events not flagged as “good” at the times of the bursts (such as those that do not enter through the PCA aperture) in the *RXTE* “Standard 1” event files. We also verified that both events were clearly detected in all operational PCUs. Hence the events are unlikely to be instrumental in origin.

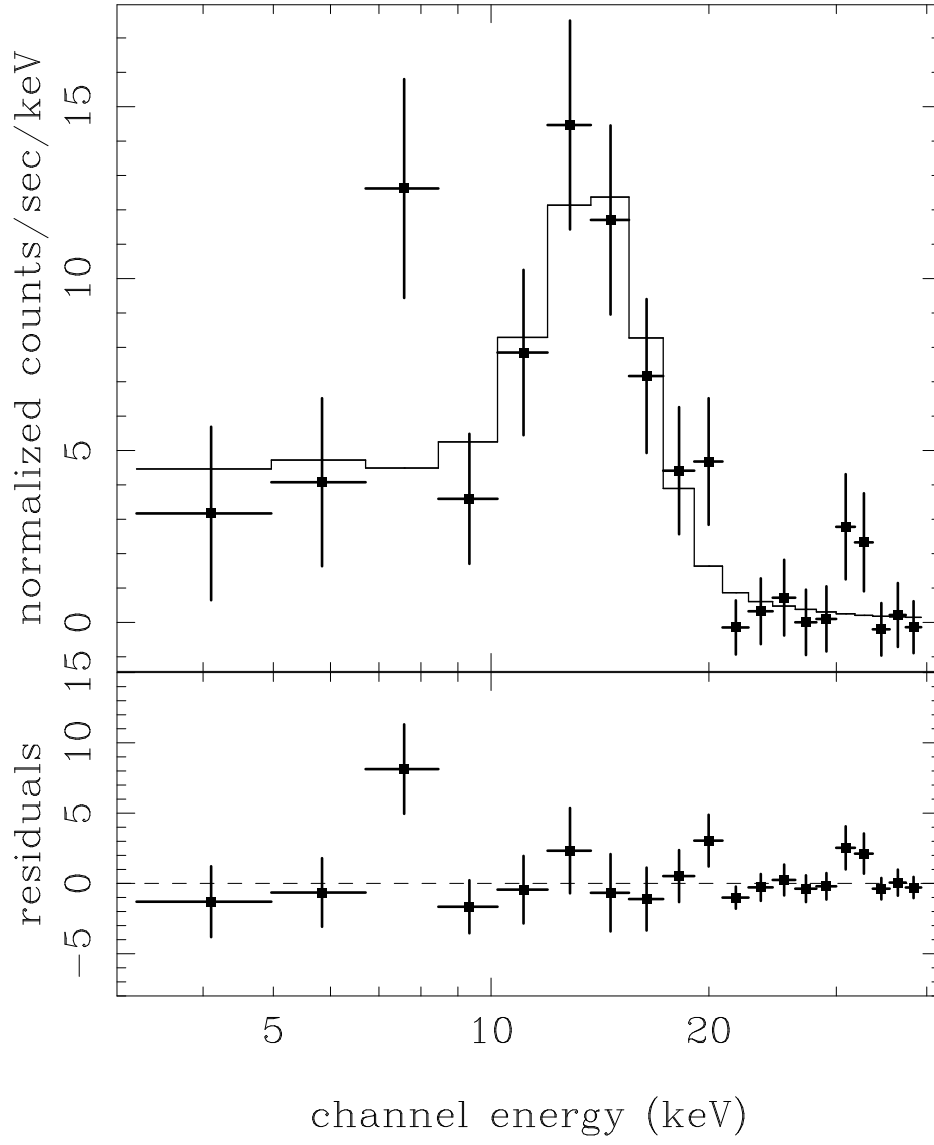


Figure 2.

Figure 2 Caption

X-ray spectrum in the 2–40 keV range for the 1 s after the onset of Burst 1. For all spectral analyses, we first created spectral files having 256 channels across the full PCA energy range (~ 0.2 –60 keV), although subsequent factor of 4 rebinning was necessary because of the paucity of burst counts. The burst and background intervals were used as input to the X-ray spectral fitting package **XSPEC**²⁶ v11.1.0². The spectrum of the first 1 s after Burst 1 onset is not well characterized by any continuum model. The best fit power-law plus Gaussian line model is shown as a solid line. The F-test shows that the addition of a line of arbitrary energy, width and normalization to a simple power law model improves the fit significantly, with a chance probability of this occurring of 0.0032. Monte Carlo simulations in **XSPEC** were done to verify this conclusion: 10,000 simulations of similar data sets were produced assuming a simple power-law energy distribution, then fit with a power law plus Gaussian line of arbitrary energy, width and normalization. This procedure is conservative, since it ignores that the observed large line has flux comparable to the measured continuum. In 10,000 trials, we found 1 trial with the same or smaller chance occurrence probability as judged by the F-test, indicating that the probability of the line we observed being due to random chance is < 0.0001 . We repeated this procedure for data having a black-body spectrum, with similar results, namely the probability of the line being due to chance is < 0.0008 . The spectrum also shows possible additional features at ~ 7 keV and ~ 30 keV (suggestive of lines at multiples of 1, 2 and 4 of ~ 7 keV). These additional features are not apparent in all binning schemes and are not statistically significant.

²<http://xspec.gsfc.nasa.gov>